CrossMark

ORIGINAL ARTICLE

Thermal strain behavior and strength degradation of ultra-high-strength-concrete

**Young Wook Lee · Gyu Yong Kim ·
Nenad Gucunski · Gyeong Choel Choe ·
Min Ho Yoon**

Abstract With the increasing application of high-strength-concrete (HSC) in high-rise-buildings for which structural safety performance is needed. However, the thermal mechanical behavior of HSC exposed to fire differs from that of normal-strength concrete (NSC). HSC is known to show different thermal strain behavior and strength degradation from NSC. It is needed to consider the thermal strain of HSC at elevated temperature under loading condition. In this study, the thermal strain behavior and strength degradation of HSC when exposed to elevated temperatures under loading conditions were examined experimentally. The compressive strength, thermal expansion, total strain, and hightemperature-creep at elevated temperatures were evaluated. To evaluate the thermal expansion of HSC at elevated temperatures, HSC with compressive strengths of 80, 130, and 180 MPa concrete were heated to 700 °C at a rate of 1 °C/min. The total strain and high-temperature-creep were measured under the loading condition of 25 % of the compressive strength at room temperature. The experimental results clearly showed that the strength degradation of HSC increased with the higher compressive strength at elevated temperature. Thermal expansion occurred consistently regardless of the strength level without loading. However, 180 MPa concrete failed while being heated to around 300 °C. The transient creep had a large influence on the high temperature-creep as the HSC was heated at elevated temperature while under a load. It is considered that the reduced amount of aggregate and increased binder content make extremely density matrix in HSC, and it is particularly evident as the compressive strength increased.

Keywords Ultra-high-strength-concrete · Thermal expansion · High-temperature-creep · Total strain

1 Introduction

Because of the increased demand for slender high-rise building structures, high-strength-concrete (HSC) with a compressive strength that exceeds 80 MPa is coming into use. Recently, HSC that can be cast-in-place and cured at ambient temperatures to develop a compressive strength that exceeds 80 MPa has been developed, and research on its practical applications is in progress [1]. Many previous studies have shown that the inside of HSC becomes denser at low water/cement ratios, and HSC shows an even greater degradation in mechanical performance compared to normal-strength concrete (NSC) at elevated temperatures [2, 3].

Y. W. Lee · G. Y. Kim (✉) · G. C. Choe · M. H. Yoon
Department of Architecture Engineering, College of
Engineering, Chungnam National University, 99
Daehak-ro Yuseong-gu, Daejeon 305-764, Korea
e-mail: gyuyongkim@cnu.ac.kr

N. Gucunski
Department of Civil and Environmental Engineering,
Rutgers University, Piscataway, NJ 08855-0909, USA

In light of this, Fu et al. [4] researched the strength degradation of hardened cement pastes (HCP) when heated that causes micro-cracks to occur from the high temperature. Li and Purkiss [5] performed a thermal strain analysis on concrete by comparing previously presented mechanical behavior models when high temperature was considered to determine the validity of these models. Schneider et al. [6] and Sabeur and Meftah [7] each evaluated NSC and HSC to verify their strain behaviors at high temperatures and with applied loads. Kodur et al. [8] suggested a mathematical model to evaluate the fire resistance of high-performance concrete (HPC) according to the loading, fiber incorporation, concrete strength, and aggregate type. In particular, Anderberg and Thelandersson [9], Harmathy [10], Lie and Irwin [11], and Guo and Shi [12] researched the high-temperature creep behavior of NSC under load conditions. Also, Kodur et al. [13], Hu et al. [14], Kang et al. [15] researched the high-temperature creep behavior of HSC

In the event of a fire, when the creep strain progresses upon the remaining resistance of the main structural members, the building structure may become irregular. Previous studies have shown that the high-temperature-creep of a concrete structure under fire conditions for 120–180 min is similar to the creep that occurs over 20–30 years under normal conditions [16]. Thus, it can significantly influence the performance of the structure. For HSC, which is used in skyscrapers, research needs to be conducted on not only the strength degradation but also the thermal expansion and shrinkage that occur under compressive stress with elevated temperature.

Therefore, the object of this paper is to evaluate how concrete with compressive strength exceeds 80 MPa behave under various temperature condition and loading condition as a baseline for fire safety.

In this study, HSC with compressive strengths of 80, 130, and 180 MPa were subjected to a wide range of temperatures from room temperature to 700 °C. The thermal expansion, total strain, high-temperature-creep at elevated temperature under a load were evaluated.

2 Experiment plan and method

2.1 Experiment plan

In this study, an experiment was performed to evaluate the thermal strain behavior and strength degradation of

HSC with compressive strengths of 80, 130, and 180 MPa. Table 1 outlines the experimental plans. Two different loading conditions of $0.00f_{cu}$, $0.25f_{cu}$ were used, and the target heating temperature conditions were set to 100, 200, 300, 500, and 700 °C. The $0.00f_{cu}$ is that the specimen is loaded by 0 % of ultimate load of the specimen at room temperature which means that it is unstressed condition. Also, $0.25f_{cu}$ means that the specimen is pre-loaded with 25 % of ultimate load of the specimen at room temperature. The evaluated parameters were the high-temperature compressive strength, thermal expansion, total strain, high-temperature-creep, and transient creep.

Figure 1 shows heating and loading scheme for the thermal expansion and total strain test according to RELEM TC 129-MHT. The thermal expansion was measured under heating conditions without loading. In total strain, the specimen is pre-loaded before heating to target temperature at a load of 25 % the compressive strength at room temperature and the total strain was measured during heating [19]. The high-temperature-creep has been measured for 300 min after the target temperature was reached, at the conditions of the constant heating temperatures and load of 25 % of the compressive strength at room temperature [19].

2.2 Concrete mix and production of specimens

In this study, type I Portland cement (C), fly ash (FA), blast furnace slag (BFS), silica fume (SF) and anhydrous gypsum (Gy) were used as binders. Table 2 lists their chemical compositions and physical properties.

HSC is frequently used for the structural members of skyscrapers; therefore, it requires an adequate pump pressure feed and decent workability. In the present study, crushed granite gravel with a specific weight of 2.70, water absorption rate of 0.9 %, and maximum size of 13 mm was used as the coarse aggregate. Sea sand with a specific weight of 2.65 and water absorption rate of 1.00 % was used as the fine aggregate. A polycarboxylic based superplasticizer was used to achieve the required workability of the concrete mixes. Table 3 lists the physical properties of these aggregates.

Table 4 presents the mix proportions for HSC used in this study. To reach compressive strengths of 80, 130, and 180 MPa, W/B was set to 20.0, 14.5, and 12.5 %, respectively. For the series I, cement (C), silica fume (SF), and fly ash (FA) were used as

Table 1 Experimental outline

Experiment factors				Test items	
W/B[a]	f_{ck} (MPa)	Preload ratio[b]	Temperature (°C)	Fresh concrete	Hardened concrete (the number of used specimens)
0.200	80.0	0.00	Room temperature[c]	Slump flow (mm)	Compressive strength
0.145	130.0	0.25	Elevated temperature (100, 200, 300, 500, 700)	Air content (%)	Room temperature
0.125	180.0				(3 specimens × 3 type of W/B × 2 curing age = 18ea)
					Elevated temperature
					(3 specimens × 3 type of W/B × 2 loading condition × 5 temperatures = 90ea)
					Thermal expansion
					(3 specimens × 3 type of W/B × 5 temperatures = 45ea)
					Total strain, High-temperature-creep
					(3 specimens × 3 type of W/B × 5 temperatures = 45ea)
					Transient creep

[a] *W/B* water-to-binder ratio

[b] Percentage of ultimate load at room temperature

[c] Approximately 20–24 °C

Fig. 1 Heating and loading schemes for test. **a** Thermal expansion, **b** Total strain
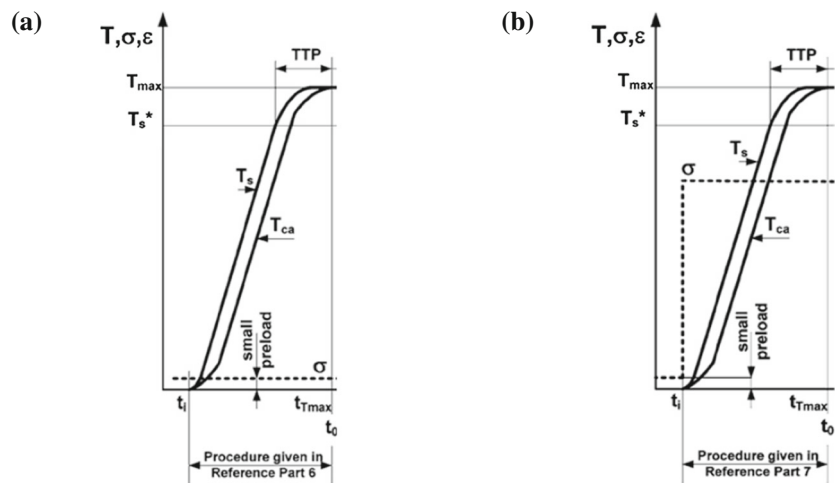
where	T	: Temperature	T_{ca}	: Temperature at central axis of rotation of specimen
	σ	: Load	T_S	: Surface temperature at which dT_s/dT
	ε	: Strain	TTP	: Transitional thermal period
	T_{max}	: Maximum temperature	T_i	: Time at initiation of test
	T_S	: Temperature at surface of specimen	T_o	: time at beginning of steady state regime

binders. For the series II and series III, C, blast furnace slag (BFS), SF, and anhydrous gypsum (AG) were used.

For f_{ck} 80.0, the fine aggregate ratio was fixed at 43 %. For f_{ck} 130.0 and f_{ck} 180.0, it was set to 35 %. The unit weight was fixed to 150 kg/m^3.

Table 2 Properties of used binders

Materials Chemical composition (%)	OPC[a]	FA[b]	BFS[c]	SF[d]	AG[e]
SIO_2	21.65	22.09	32.75	95.30	0.73
AL_2O_3	5.41	5.24	13.78	0.06	0.17
Fe_2O_3	3.24	3.52	0.42	0.02	0.16
CaO	63.37	63.57	43.51	0.16	41.57
MgO	2.28	2.18	3.8	0.3	–
SO_3	2.04	2.03	5.23	–	55.5
K_2O	1.04	0.95	0.49	0.31	0.03
Loss on ignition (%)	0.97	3.99	–	–	–
Density (g/cm^3)	3.15	2.2	2.90	2.5	2.5
Specific surface (cm^2/g)	3200	3000	6000	2×10^5	3550

[a] *OPC* ordinary Portland cement

[b] *FA* fly ash

[c] *BFS* blast furnace slag

[d] *SF* silica fume

[e] *AG* anhydrous gypsum

Before the specimens were produced, properties of the fresh concrete such as the slump flow and air volume were evaluated. The slump flow was measured by referring to KS F 2402 [17], and the air volume was measured by referring to KS F 2421 [18]. All of the concrete types had a slump flow of 750 ± 100 mm and air volume of 2 ± 1 %.

With each mixture, cylindrical specimens were casted by steel molds of size 100×200 mm. 24 h after their preparation, they were cured in tap water at 20 ± 2 °C. The specimens for the compressive strength test at an age of 28 days were cured in the water for 28 days. The specimens for the heating test were cured in water until an age of 7 days and subsequently cured in a climate room at a temperature of 20 ± 2 °C and a relative humidity of 50 ± 5 %

during 300 days. Then, a heating test was performed. The standard water content at 300 days for f_{ck} 80.0, f_{ck} 130.0, and f_{ck} 180.0 was measured as under 3.00 % which is 2.50 ± 0.40 %, respectively.

In this study, 108 specimens for compressive strength at room temperature and elevated temperature, 45 specimens for thermal expansion strain, and 45 specimens for total strain and high temperature creep were made and tested, respectively. The number of used specimens in this study is shown in Table 1, and the total number of used specimens is 198. The compressive strength of the specimens used in this study is shown as Table 5.

2.3 Testing method

In this study, for each set of tests at a given temperature, three specimens from the same batch were used. The test equipment for heating and loading is shown in Fig. 2. For simultaneous loading and heating, an electric heating furnace was installed loading apparatus with a capacity of 2000 kN. Furthermore, the strain of the test specimens during heating was measured by transferring the strain to the displacement meter placed outside through a quartz

Table 3 Physical properties of aggregates

Properties	Fine aggregate	Coarse aggregate
Maximum size (mm)	5	13
Fineness modulus	2.9–3.1	6.91
Specific gravity (g/cm^3)	2.65	2.70
Water absorption (%)	1.00	0.90

Table 4 Mix proportions of high-strength-concrete

W/B	Slump flow (mm)	S/a (%)	Air (%)	Unit weight (kg/m^3)							
				W	C	BFS	SF	FA	AG[a]	S	G
0.200	750 ± 100	43.0	2 ± 1	150	525	0	75	150	0	644	870
0.145		35.0			652	207	124	0	52	448	848
0.125		35.0			660	240	240	0	60	389	736

[a] *AG* anhydrous gypsum

Table 5 Compressive strengths of high-strength-concrete at elevated temperature and room temperature

W/B	Preload ratio[a]	Room temperature[b]		Compressive strength(MPa) at elevated temperature (300 days)				
		28 days	300 days	100 °C	200 °C	300 °C	500 °C	700 °C
0.200	0.00	77.21	81.85	72.11	82.79	74.64	46.56	34.33
		75.59	83.24	75.68	85.33	71.12	47.48	37.59
		75.20	83.88	75.08	84.33	72.85	50.23	36.62
	0.25	–	–	77.41	83.17	66.88	64.11	54.45
		–	–	78.89	80.47	63.15	63.34	52.11
		–	–	79.50	85.18	64.16	62.75	52.20
0.145	0.00	124.47	136.73	96.29	126.46	119.98	60.51	25.42
		126.66	132.22	90.48	129.39	125.80	63.66	21.92
		123.87	135.54	90.37	130.40	124.48	60.39	20.52
	0.25	–	–	86.68	107.71	102.79	66.61	52.99
		–	–	87.12	103.59	107.38	65.82	57.56
		–	–	83.60	102.14	109.78	65.27	54.09
0.125	0.00	178.55	185.85	113.47	170.83	F[c]	F[c]	F[c]
		177.79	186.41	106.26	164.00	F[c]	F[c]	F[c]
		174.60	181.24	109.91	163.56	F[c]	F[c]	F[c]
	0.25	–	–	119.98	159.98	137.77	64.27	38.87
		–	–	125.77	157.65	138.67	58.88	36.89
		–	–	123.70	153.91	136.27	56.28	32.24

[a] Stress ratio = load/compressive strength at room temperature

[b] Room temperature: approximately 20–24 °C

[c] Fractured during the test

tube of ø100 mm in diameter, which penetrated the center of the upper and lower loading jigs.

To increase the temperature inside and outside of the test specimens to the same level, an indirect heating method was used in which heat was transferred to the test specimens by heating the upper and lower loading jigs. The specimens were encased in heat transmission jig and heat transfer cover to heat the whole specimen indirectly and to increase the temperature inside and outside of the test specimens with the same level as shown in Fig. 2c.

Figure 3 shows the heating and measuring of temperatures. To measure representative temperature and to control furnace temperature, three type-K Chromel–alumel thermocouples, 0.91 mm thick, were installed in testing specimens. On the surface of specimen, two thermocouples were installed at top–bottom height (10 mm from top and bottom, 5 mm from surface) of the cylinder and one thermocouple was installed at mid-height. On the center of specimen, two thermocouples were installed at top–bottom

height (25 mm from top and bottom, 50 mm from surface) of the cylinder and one thermocouple was installed at mid-height as shown in Fig. 3. Also, the heating temperature of furnace was controlled from electric heater by voltage feedback-type thyristor regulator system. Every specimen for each test at elevated temperature was heated at a rate of 1 °C/min, and it was confirmed that the standard temperature variation between inside and outside of the specimen was under 5 °C [19].

After specimen reached the target temperature, the temperature was maintained for 30 min, and then compressive strength was tested.

The strain of the specimen was calculated according to Eq. (1).

$$\Delta L_c = \Delta L_2 - \Delta L_1 \tag{1}$$

where ΔL_c is the thermal strain of concrete (mm), ΔL_1 is the measured strain of the upper LVDT (mm), and ΔL_2 is the measured strain of the lower LVDT (mm).

Fig. 2 Test equipment for heating and loading. **a** 2,000kN UTM, **b** Electric heating furnace, **c** Heat transmission jig
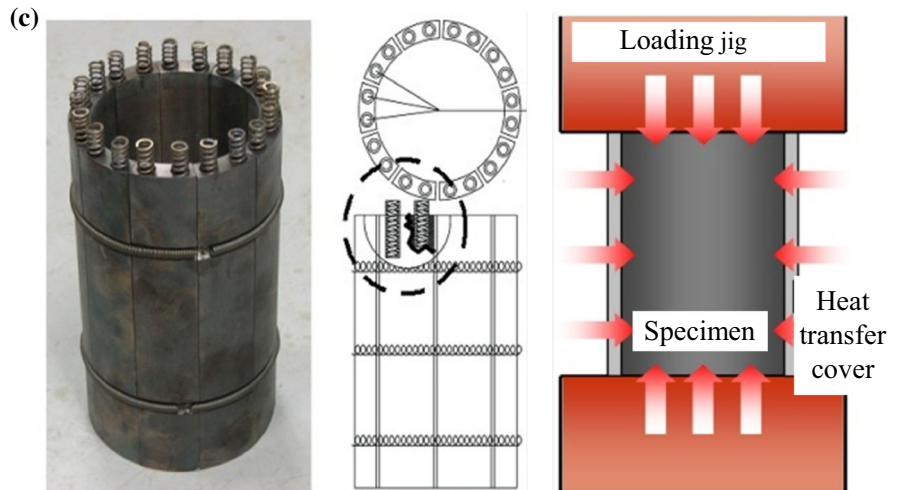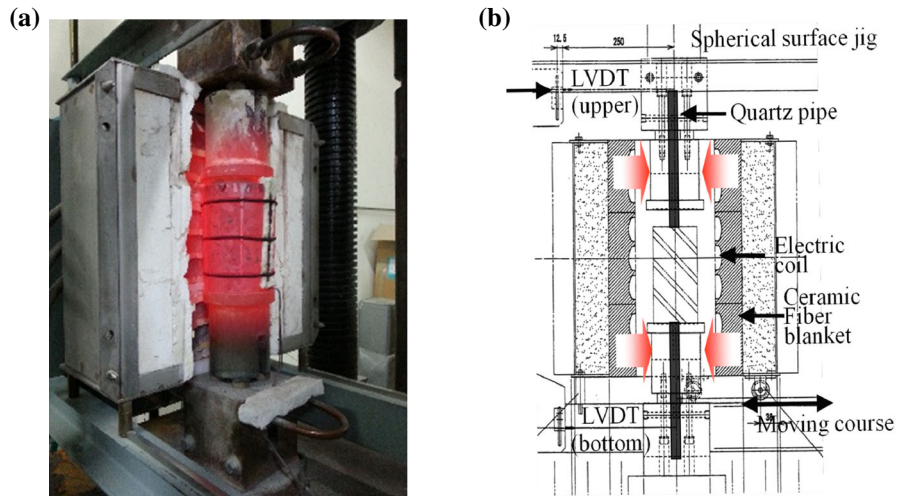
Fig. 3 Heating and measuring method of temperature (heating velocity: 1 °C/min., temperature variation of surface and center of specimen: under 5 °C)
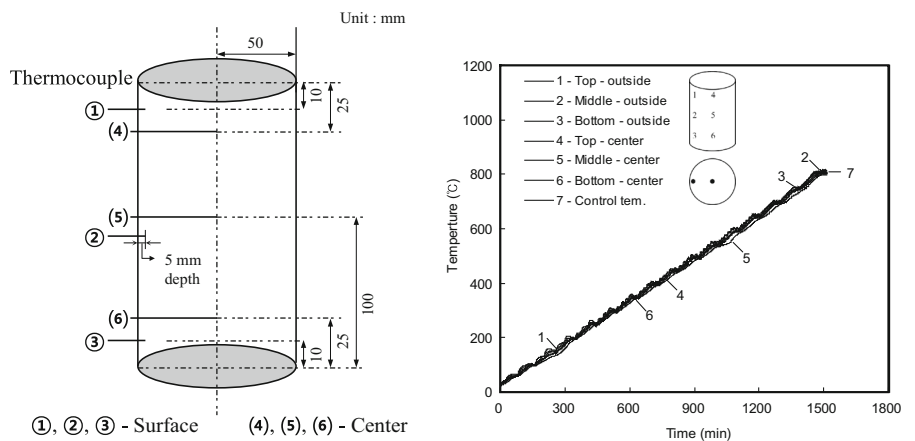
3 Test results and considerations

3.1 Thermal expansion

Figure 4 shows the thermal expansion of HSC depending on the temperature. The thermal expansion tended to increase with the temperature. When the temperature was over 600 °C, the thermal expansion plateaued at 0.009. At 700 °C, the strain increased by less than 0.001. When the temperature was below 300 °C, specimens with different strengths showed similar strains without significant differences. However, f_{ck} 180.0 failed when it was heated to around 300 °C, so the thermal expansion could not be measured beyond that point. Compared to the CEN and CEB codes based on previous research, the actual strain was measured at 0.002 less when the temperature was 600–700 °C.
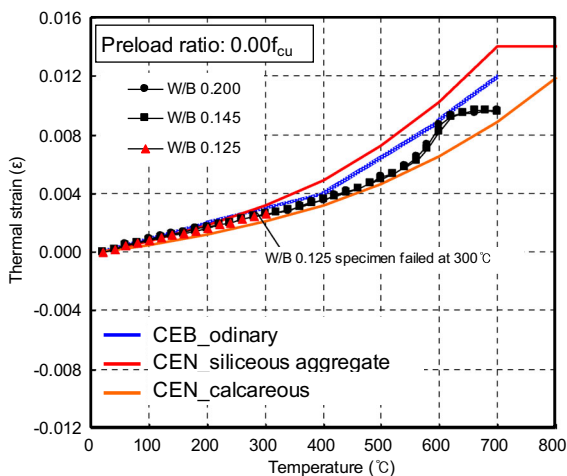
3.2 Total strain

Figure 5 shows the total strain of HSC depending on the temperature. The total strain was when a load and heat were applied at the same time. The experiment took the same amount of time as the one on the thermal expansion. The reason for the significant reduction of the thermal expansion was the offsetting effects caused by the load. For f_{ck} 80.0, the thermal expansion was restrained. However, the expansion force of the aggregate maintained the total strain at 0.001. The specimen shrunk at temperatures above 600 °C; thus, the thermal expansion was offset. For f_{ck} 130.0 and f_{ck} 180.0, the thermal expansion was offset above 100 °C. The shrinkage strain gradually appeared above 300 °C. When the temperature was above 600 °C, which produces a change in the concrete state, a shrinkage strain occurred abruptly. The total strain was -0.008 at 700 °C.

Meanwhile, the reason that f_{ck} 130.0 and f_{ck} 180.0 were not fractured even with a significant total strain of -0.006 at 700 °C during the application of a 0.25 f_{cu} load was because energy dissipation became possible in the ductile state as the shrinkage cracks adjusted to the load. The resistance gradually decreased in accordance with the thermal expansion of the aggregate, which allowed the energy to dissipate when the concrete was in the ductile state.

Unlike the thermal expansion, where specimens of different strengths showed similar results, the total strain tended to decrease at high temperatures as W/B decreased. Figure 6 shows the initial load corresponding to 25 % of the compressive strength at room temperature along with the Rs(T) ratio, which is the compressive strength at each corresponding temperature ($f_{c,T}$). The compressive strength have been decreased with increasing temperature and decreasing W/B. Therefore, even though a load corresponding to 25 % of the compressive strength at room temperature was applied equally, the rate of decrease in the compressive strength greatly increased for lower W/B as the temperature increased. The greater load rates at elevated temperatures were assumed to result in a significant shrinkage of the total strain for lower W/B.

**Fig. 4** Thermal expansion of high-strength concrete
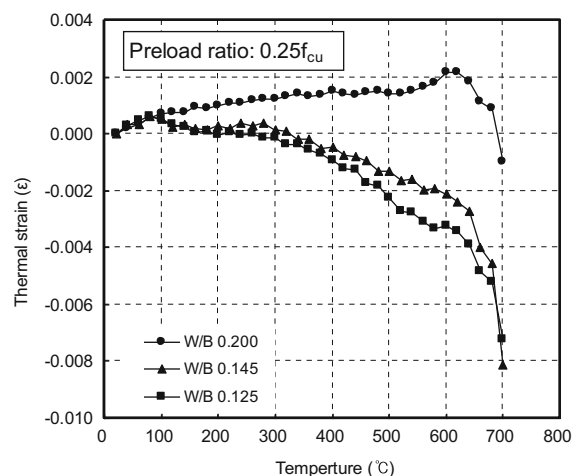
Fig. 5 Total strain of high-strength-concrete
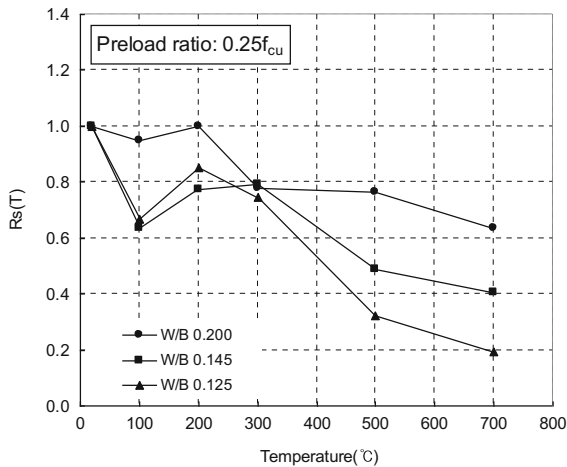
Fig. 6 Strength ratio of $0.25f_{cu}$ load/strength at each temperature

Figure 7 shows the stress–strain curve depending on the temperature and stressed conditions. For non pre-loaded condition, specimens have been heated to target temperature without loading and then loading have been applied to specimens when specimen reached target temperature. Under the non pre-loaded condition, f_{ck} 80.0 and f_{ck} 130.0 showed an almost linear stress–strain curve for strains below 0.004 up to a temperature of 300 °C. However, beyond 500 °C, the slope lowered, and the strain became 0.01 at 700 °C. For f_{ck} 180.0, the strain were similar when the temperature was below 200 °C. Above 300 °C, the concrete failed with the application of heat, so measuring the high-temperature compressive strength was impossible.

For pre-loaded condition, pre-loaded specimen at a 25 % load of compressive strength have been heated to target temperature and then loading have been applied to specimens when specimen reached target temperature. Under the pre-loaded condition, the specimen showed a small strain when it failed at elevated temperatures above 500 °C. The slope increased with the compressive strength of the HSC, and the majority of the specimens had a strain ratio of 0.003–0.004 when they finally failed. It means that, at elevated temperatures above 500 °C, cracking occurred in the interfacial transition zone between the cement paste and aggregate, which lowered the resistance. However, the cracking was suppressed by the load, which caused shear failure to also occur at elevated temperatures.
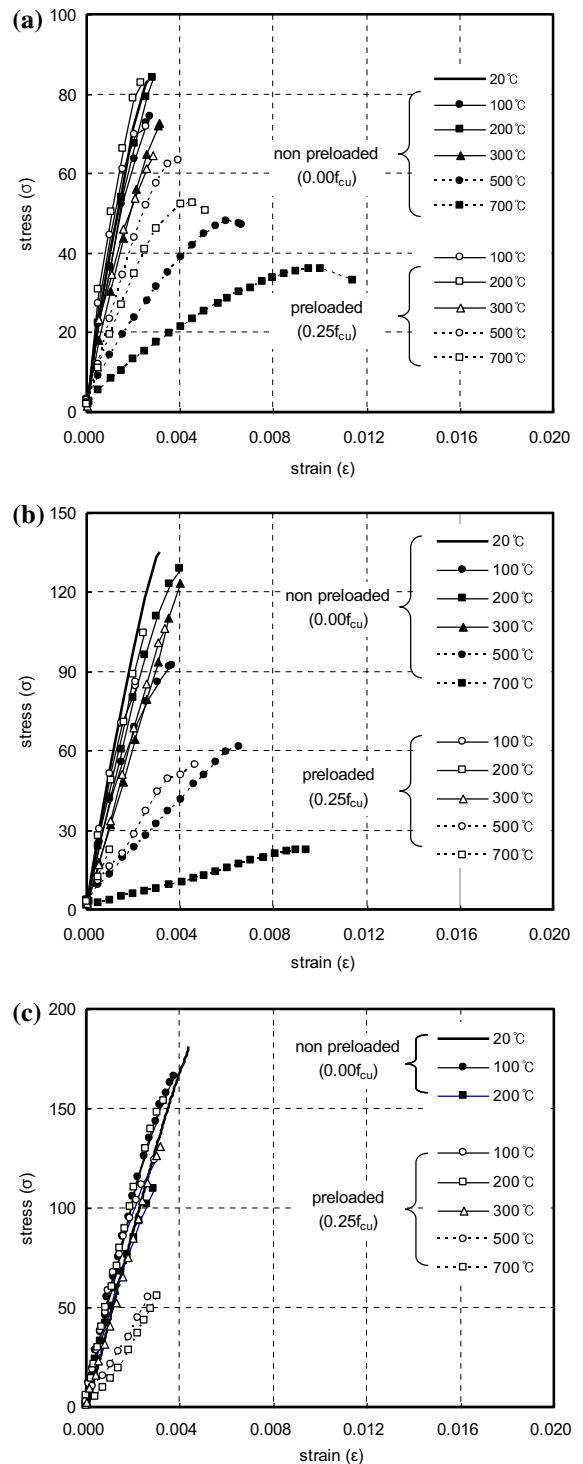
Fig. 7 Stress-strain curve under elevated temperature and loading conditions. **a** W/B 0.200, **b** W/B 0.145, **c** W/B 0.125

Figure 8 shows the transient creep of HSC depending on the load and temperature. The transient creep is the shrinkage strain that occurs because of the load and occurs when the state of concrete changes as the temperature increases and the resistance lowers.

When a load of $0.25f_{cu}$ was applied to f_{ck} 80.0 concrete, the transient creep increased below 300 °C. Shrinkage occurred very rapidly at temperatures above 500 °C because of the influence of the load. At 700 °C, the transient creep was 0.011, which was similar to the values of the thermal strain without a load.

For f_{ck} 130.0 and f_{ck} 180.0, the final transient creep above 700 °C was 0.017, which was greater than that for f_{ck} 80.0.

In this research, the compressive strength of HSC greatly decreased above 300 °C. This is because the coarse aggregate had a small maximum size, and a large amount of the specimen comprised powdery components. Thus, applying high temperatures and a load decreased the cohesion of the concrete matrix, which caused an abrupt shrinkage strain.

3.3 High-temperature-creep

Figure 9 shows 5 h of high-temperature creep for the HSC concrete as evaluated according to the high-temperature-creep test method [19]. The figure shows the high-temperature-creep at 700 °C for f_{ck} 180.0; compressive fracture occurred from the load (σ) during the test.
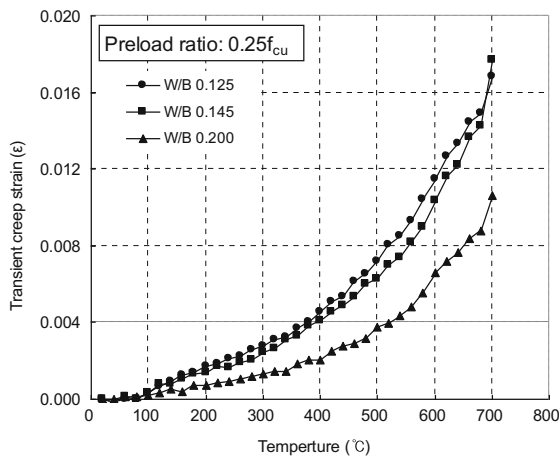
The high-temperature-creep of HSC increased with the temperature regardless of W/B. Very high-speed high-temperature-creep behavior occurred in the first
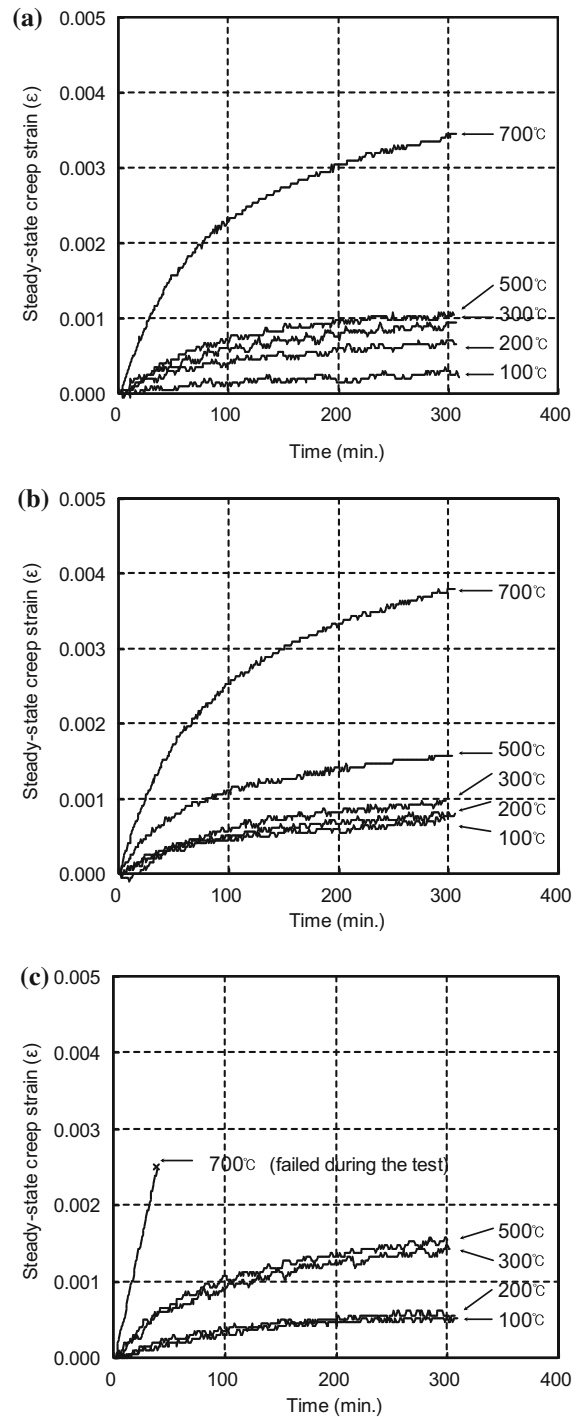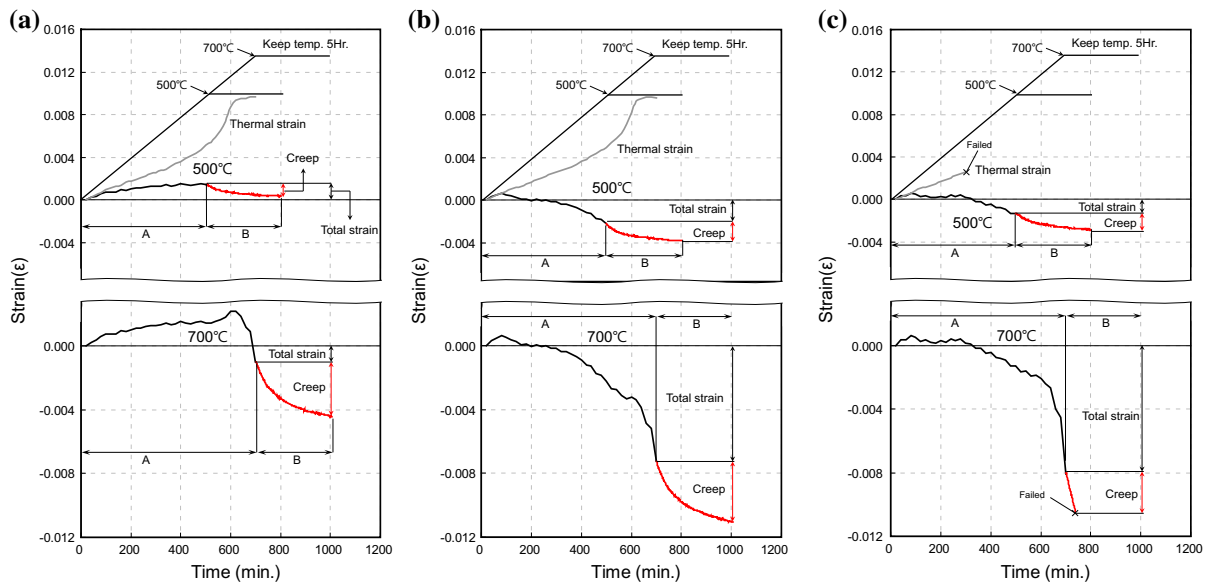

Fig. 8 Transient creep of high-strength-concrete

Fig. 9 High-temperature-creep of high-strength-concrete at elevated temperature. **a** W/B 0.200, **b** W/B 0.145, **c** W/B 0.125

Fig. 10 Total strain and high-temperature-creep of high-strength-concrete with elevated temperature of 500, 700 °C under $0.25f_{cu}$ loading. **a** W/B 0.200, **b** W/B 0.145, **c** W/B 0.125

50 min. The strain gradually decreased after that. When the temperature was below 500 °C, about 80 % of the high-temperature-creep over 300 min was caused by the shrinkage in the initial 100 min. The specimen then showed a constant strain value. Above 500 °C, over 60 % of the high-temperature-creep of 300 min was caused by creep shrinkage in the initial 100 min. After that, the shrinkage rate decreased, but a significant amount of creep continued to occur.

A small high-temperature-creep of approximately 0.002 occurred at temperatures up to 500 °C during the 5 h of the creep test. However, there was a clear difference in high-temperature-creep at 700 °C (see Fig. 9a). The high-temperature-creep was about three times larger at 700 °C compared to below 500 °C. The strain behavior of the high-temperature-creep greatly increased at lower W/B ratios. This is because creep is linearly proportional to the axial ratio ($\sigma/f_{c,T}$); thus, it helps cause the total strain, as noted previously (Fig. 6).

Figure 10 shows the total strain and high-temperature-creep of high-strength-concrete with elevated temperature of 500, 700 °C and 0.25 f_{cu} loading. Section A is the total strain depending on the temperature, and Section B is the high-temperature-creep over time at a maintained temperature of 700 °C. For f_{ck} 80.0, high-temperature-creep at 700 °C was 0.0035. This is 3.5 times larger than

0.001, which was the total strain. The final strain was 0.0044; thus, the high-temperature-creep constituted approximately 80 % of the final strain. For f_{ck} 130.0, the high-temperature creep at 700 °C was 0.0035. This is about half the total strain, which was 0.0073. The final strain was 0.011, so the high-temperature-creep was about 35 % of the final strain. The f_{ck} 180.0 showed an abrupt high-temperature-creep at the beginning of the test and failed before the temperature could reach 700 °C.

4 Conclusion

The results with regard to the thermal strain behavior and strength degradation of HSC are as follows:

(1)   Thermal expansion occurred in HSC consistently regardless of the compressive strength. However, when a load of 25 % of the design standard strength was applied, the thermal expansion from the application of heat was suppressed at higher strengths, and shrinkage from resisting force deterioration soon occurred. This phenomenon clearly increased above 130 MPa concrete. Especially the 180 MPa concrete failed from the thermal strain while being heated to around 300 °C.

(2) The transient creep had a large influence on the high-temperature-creep as the HSC was heated to the target temperature while under a load. The transient creep particularly increased when the strength was over 130 MPa concrete at high temperatures of over 500 °C. Therefore, the transient creep must be considered when evaluating the high-temperature-creep of HSC.

(3) The resisting force of HSC to withstand a certain amount of load rapidly deteriorated when it was heated to high temperatures. This is because of the reduced amount of aggregate and increased binder content which make extremely density matrix in the concrete for higher compressive strength development. In other words, resistance properties of concrete to high temperature is degraded when there are more binders with a high rate of thermal decomposition and shrinkage. This phenomenon was particularly evident as the compressive strength increased.

(4) HSC has the great advantage of providing structural stability to a building because of its high material strength. However, the risk of fire needs to be considered because its resistance sharply decreases when exposed to high temperatures. While this is beyond the scope of this research, the thermal expansion of the material also needs to be considered by evaluating the material properties and heat capacity of the HSC components under applied heat and load conditions.

References

1. Lee JH, Sohn YS, Lee SH (2012) Fire resistance of hybrid fibre-reinforced, ultra-high-strength concrete columns with compressive strength from 120 to 200MPa. Mag Concrete Res 64:539–550

2. Kim GY, Kim YS, Lee TG (2009) Mechanical properties of high-strength concrete subjected to high temperature by stressed test. Trans Nonferrous Metals Soc China 19:128–133

3. Schneider U (2007) Recommendation of RILEM TC 200-HTC: mechanical concrete properties at high temperatures—modeling and application. Part 11: relaxation. Mater Struct 40:449–458

4. Fu YF, Wong YL, Poon CS et al (2004) Experimental study of micro/macro crack development and stress–strain relations of cement-based composite materials at elevated temperatures. Cem Concr Res 34(5):789–797

5. Li LY, Purkiss J (2005) Stress–strain constitutive equations of concrete material at elevated temperatures. Fire Saf J 40(7):669–686

6. Schneider U., Schneider M, Franssen JM (2008) Consideration of nonlinear creep strain of siliceous concrete on calculation of mechanical strain under transient temperatures as a function of load history. In Fifth International Conference Structures in Fire, pp 463–476

7. Sabeur H, Meftah F (2008) Dehydration creep of concrete at high temperatures. Mater Struct 41(1):17–30

8. Kodur VKR, Wang TC, Cheng FP (2004) Predicting the fire resistance behaviour of high strength concrete columns. Cement Concr Compos 26(2):141–153

9. Anderberg Y, Thelandersson S (1976) Stress and deformation characteristics of concrete at high temperatures. 2. Experimental investigation and material behaviour model. Bulletin of Division of Structural Mechanics and Concrete Construction 54p.

10. Harmathy TZ (1983) Fire severity: basis of fire safety design. ACI Special Publication, Detroit

11. Lie TT, Irwin RJ (1995) Fire resistance of rectangular steel columns filled with bar-reinforced concrete. J Struct Eng 121(5):797–805

12. Guo ZH, Shi XD (2003) Behaviour of Reinforced Concrete at Elevated Temperature and its Calculation. Tsinghua University Pressing, (**in Chinese**)

13. Kodur VKR, Sultan MA (2003) Effect of temperature on thermal properties of high-strength concrete. J Mater Civ Eng 15(2):101–107

14. Haitao HU, Yuli D (2002) Experimental research on the transient thermal strain of high strength concrete at elevated temperature. J Buil Struct 4:6

15. Kang SW, Hong SG (2003) Behavior of concrete members at elevated temperatures considering inelastic deformation. Fire Technol 39(1):9–22

16. Wu B, Lam ESS, Liu Q et al (2010) Creep behavior of high-strength concrete with polypropylene fibers at elevated temperatures. ACI Mater J 107(2):176–184

17. Korean Standards (2007) Method of test for slump of concrete. KS F 2402

18. Korean Standards (2006) Method of test for air content of fresh concrete by the pressure method (air receiver method). KS F 2421

19. Part 8: steady-state creep and creep recovery for service and accident conditions. Mater Struct **33**(1): 6–13